7 - 12 SEPTEMBER 2014, KRAKÓW
FORUM ACUSTICUM

Statistical analysis of ultrasonic signals backscattered from heated tissue phantom and soft tissue samples *in vitro*

Eleonora Kruglenko
Institute of Fundamental Technological Research Polish Academy of Sciences, Poland.

Barbara Gambin
Institute of Fundamental Technological Research Polish Academy of Sciences, Poland.

Summary
The work concerns in finding the ultrasonic characteristics of temperature changes within the heated region of two types of samples: phantom sample made from PVA (Polyvinyl Alcohol Cryogel) and soft tissues sample in vitro. We are looking for changes in the statistical parameters of the backscattered signals registered during two different heating procedures for the two types of samples. We are looking for statistical distributions describing the statistics of the signal envelope received during the experiments heating/cooling. Matching of the histogram to the different probability density functions of Rayleigh, Gamma, Nakagami and K-distribution was analyzed by calculating the mean square error. Besides, the dependence on temperature changes of characteristic parameters for considered distributions have been calculated. We conclude that the shape parameter of K-distribution is the best statistical marker of a temperature level in the performed experiments.

PACS no. 87.50.wp, 43.35.+d, 87.57.-s

1. Introduction

B-scan image, see Fig. 1, did not carry any information of structural changes during thermal process for sub-ablation temperature level, so there is a strong need to find such changes in other properties in backscattered signal. then magnitude of signal amplitude.

The aim of the paper is to prove the statement that there are changes in statistics of backscattered signal which, in a quite precise way, are predictive of temperature changes inside soft tissue samples *in vitro* as well as in its phantoms. The ultrasound backscattered signal registrated during sonification has a statistical nature because it is formed from randomly distributed scatterers located inside the medium. So, statistical properties of a signal are strongly connected with the properties of the random scatterers distribution and their reflectivity. Taking into account the fact that during temperature increase/decrease some microstructural changes in the sample must take place we are able to link the changes of temperature level and changes of the properly chosen statistical characteristics of the signal envelope. The paper concerns in finding the ultrasonic characteristics of temperature changes within the heated region of two types of samples and two different heat sources. At first, we perform heating and cooling process on the soft tissue, mimicking material, made from PVA (Polyvinyl Alcohol Cryogel). Its acoustic properties are similar to the acoustic properties of the soft tissue, because PVA has special kind of microstructure with multilevel organization. The thermal behaviour is also enough stable up to c/a 50° C. Next, soft tissue samples *in vitro* has been heated by an ultrasonic beam with the transducer of two different powers. Parallel, during heating the scanning of the sample has been made with the help of other transducer and the data has been collected with STA. The statistical analysis of RF signals envelope has been performed in two step. First, the histograms of envelope with different probability distribution functions from the set of distributions: Rayleigh , Gamma, K and Nakagami was compared. This distributions were already used for the characterization of soft tissues and their phantoms, cf. [1,2]. Secondly, the choice of

the best parameter evaluating the temperature change will be based on two criteria: the histogram matching and the strongest sensitivity of their parameter to temperature changes at different thermal processes and different materials samples.

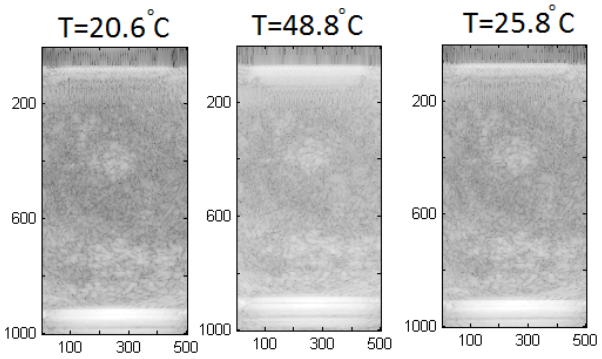

Figure 1a. B-mode image of PVA-c phantom in different temperature levels, from left to right: image 1 at the beginning of experiment - 20.6°C, image 2 after 1 hour of heating, the temperature - 48.8°C, and image 3 the end of the experiment (after 2 hours of cooling) - 25.8°C.

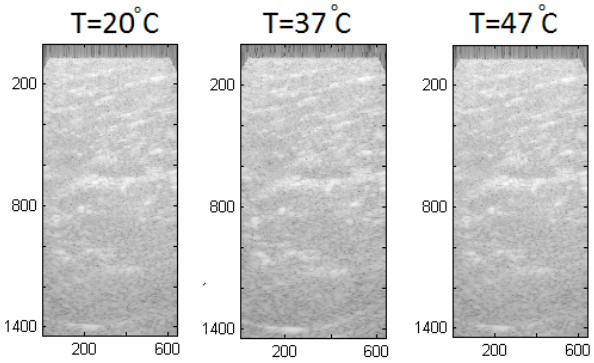

Figure 1b. B-mode image of soft tissue sample in different temperature levels, from left to right: image 1 at the beginning of experiment - 20.6°C, image 2 after 10 min of heating with power 4W, the temperature - 37°C, and image 3 after 10 min of heating with power 6W°C, temperature - 47°C.

2. Experiments

The sample made from PVA-c, 40mm x 40mm x 8mm, has been immersed into a water bath and subjected to uniform heating. The thermostat was set so that within one hour the water temperature increased linearly from 20.6°C to 48.8C°, registered by the thermometer, see Fig. 1. When disabled subsequent heating the temperature of the water after two hours, cooled to 25.8°C. Let underline that the whole volume of sample was uniformly heated. The temperature distribution during heating/cooling process within the sample was calculated using FEM program Abaqus 6.12 software (DS Simulia Corp.)., see Fig. 2, cf. [3-5].

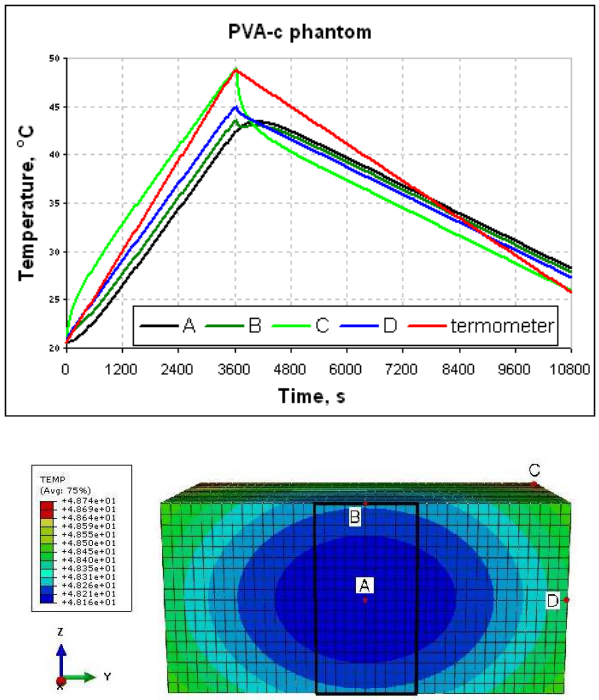

Figure 2. Temperature as function of time during heating/ cooling process for PVA. The upper: plot of the calculated temperature after 1 hour of heating and 2 hours of cooling in different points of the sample, shown in the figure the lower. Black line isolates area scanned by ultrasound transducer.

Backscattered ultrasound signals have been collected by the use of transducer L14-5/38 ULTRASONIX at a frequency of 8 MHz (ULTRASONIX SonixTOUCH, British Columbia, Canada). Pulse transmitted has 2 periods of the sine wave (pulse duration of 0.25 microseconds). To collect the data the Synthetic Transmit Aperture – STA- has been used, cf. [6,7]. With the method, an ultrasonic signal is transmitted by a single transducer and receiving echoes are registered by all elements of the transducer array. Focusing takes place in every point B-mode data.

The system for heating the soft tissue samples *in vitro* consists of generator (Agilent 332, Aprings Colorado, USA), amplifier (ENI 1325LA, Rochester NY, USA), spherical ultrasonic transducer (central frequency 2.2 MHz, diameter 44 mm, 44.5 mm focal length, area S = 15.2 cm^2) and oscilloscope (Tektronix TDS3012B), see Fig. 3.

Irradiation with two different powers: of 4 and 6W have been performed. During 10 minutes of heating and 10 minutes of cooling the temperature changes were recorded using thermocouples and registered by the USB module -TEMP.

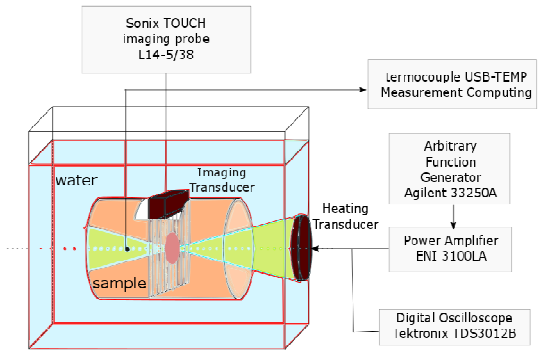

Figure 3. Scheme of soft tissue samples heating experiment.

The temperature within the sample has been measured along the beam axis at different distances from the head. The geometrical focus was located c/a 25 mm of the surface of the transducer, while the maximum temperature observed in the pattern was at a distance of 25 mm, so practically the same. The linear transducer (L14-5/38) located across the heating beam at a distance of 25 mm from the transmitter has been used to produce images during heating by the focused transducer. In this case, the heated volume is concentrated near the focusing area inside the sample and the temperature distribution is inhomogeneous.

Below, the temperature changes in different distances from transducer inside the sample and different power of heating are depicted, cf. Fig. 4, 5, 6.

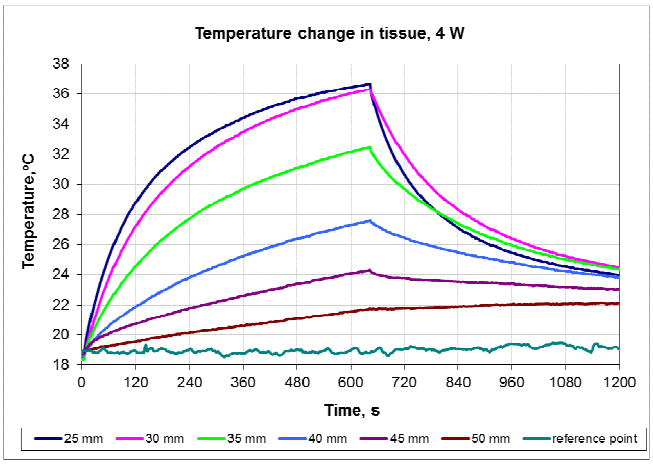

Figure 4. Temperature variation in time measured by thermocouples along the acoustic axis at various distances from transducer for soft tissue, power applied to the head 4W.

All calculations in the paper are done within Matlab (The Mathworks Inc., Natick, Massachusetts, USA) version R2014a.

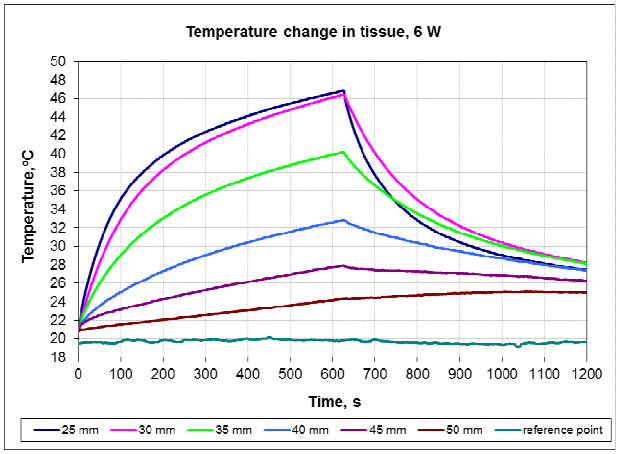

Fig. 5. Temperature variation in time measured by thermocouples along the acoustic axis at various distances from transducer, soft tissue of power applied to the head 6W

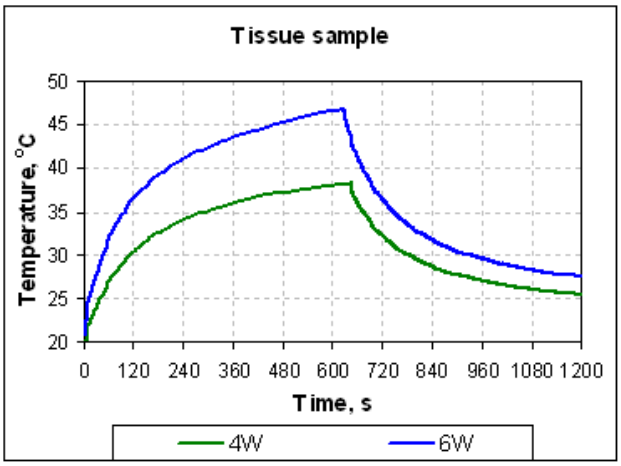

Figure 6. The experimentally determined temperature changes in the point of focus (the highest heating) in the tissue sample as a function of time / two values of power applied to the head, 10 min heating and 10 min cooling.

3. Statistical analysis

The Rayleigh distribution is one parametric, other considered here probability distributions functions (PDF) are two-parametric. Below we give formulae for the probability density functions of all distributions and on Fig 7-10 sensitivity on the parameters values on the shape of PDF's are shown. The Rayleigh distribution is one parametric, other considered here probability distributions functions (PDF) are two-parametric.

Below we give formulae for the probability density functions of all distributions and on Fig Nos. sensitivity on the parameters values on the shape of PDF's are shown.

Rayleigh distribution is defined by

$$P_{Ra}\left(A\middle|\sigma^2\right)=\frac{A}{\sigma^2}\exp\left(-\frac{A^2}{2\sigma^2}\right) \qquad (1)$$

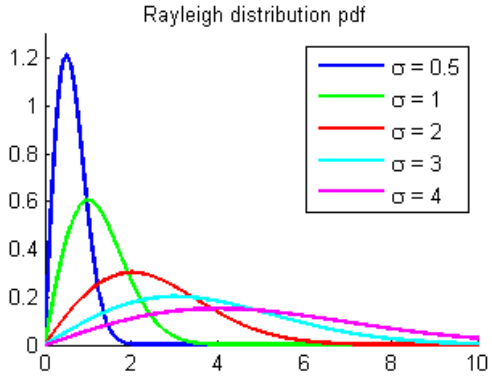

Figure 7. The probability density function of the Rayleigh distribution

Gamma distribution

$$P_G = (A|k,\theta) = \frac{1}{\Gamma(k)\theta^k} A^{k-1} e^{-A/\theta} \qquad (2)$$

where $k,\theta > 0$ shape and scale parameter, Γ is the Euler gamma function.

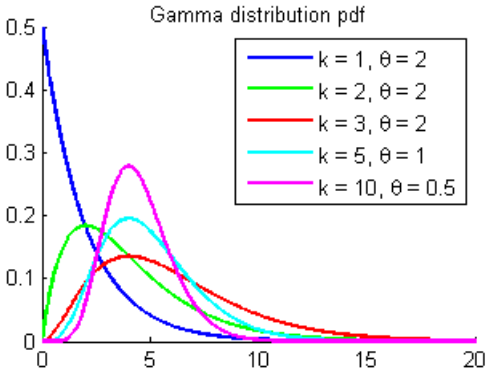

Figure 8. The probability density function of the Gamma distribution

Nakagami distribution

$$N(A|m,\Omega) = \frac{2m^m}{\Gamma(m)\Omega^m} A^{2m-1} e^{-mA^2/\Omega}, \qquad (3)$$

where $m > 0, \Omega > 0$ is the shape and the scale parameter, respectively, Γ is the Euler gamma function.

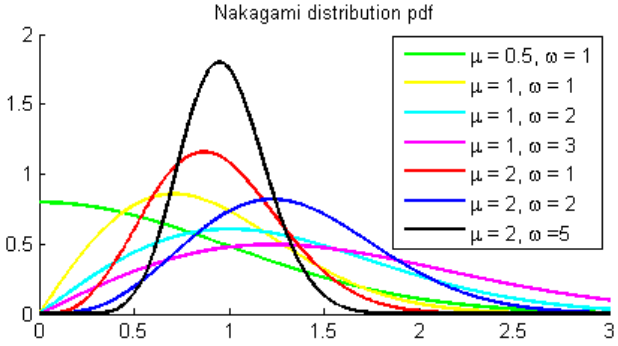

Figure 9. The probability density function of the Nakagami distribution

The K-distribution is defined by

$$P_K(A|\sigma^2,\alpha) = \frac{4A^\alpha}{(2\sigma^2)^{(\alpha+1)/2}\Gamma(\alpha)} K_{\alpha-1}\left(\sqrt{\frac{2}{\sigma^2}}A\right), \qquad (4)$$

where $\alpha > 0$, $\sigma > 0$ is the shape and the scale parameter, respectively, Γ is the Euler gamma function, and K_p denotes the modified Bessel function of the second kind of order p.

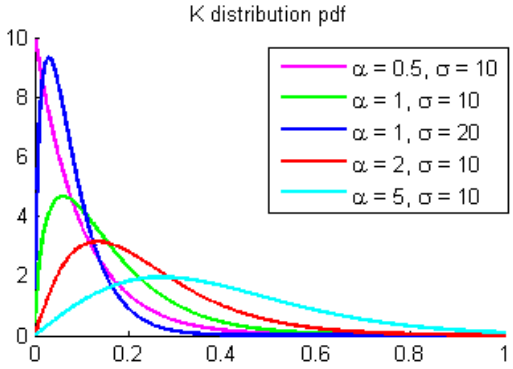

Figure 10. The probability density function of the K distribution

Fitting the histograms of envelopes to different PDF's for all experiments in two points of heating process, namely the beginning and the maximal temperature level, are shown in Fig. 11-Fig.13.

Also the quality of fitting is measured by MSE calculations, see Tab. 1, 2 3.

The temperature dependencies on four parameters, which characterized the shape of considered distributions for all experiments are shown in Fig. 14.

4. Result

The choice of the best parameter evaluating the temperature change has be based on two criteria: the histogram matching and the strongest sensitivity to temperature changes at different thermal processes and different materials samples. We conclude that Gamma distribution is the best PDF not only as fitting to histograms, but also its shape parameter is the most accurate measure of the temperature increase/decrease. But the shape parameter of Gamma distribution has no physical interpretation, contrary to the shape parameter of K-distribution, cf. [1,8-9], which is interpreted as a measure of a "number of effective scatterers" in a resolutio

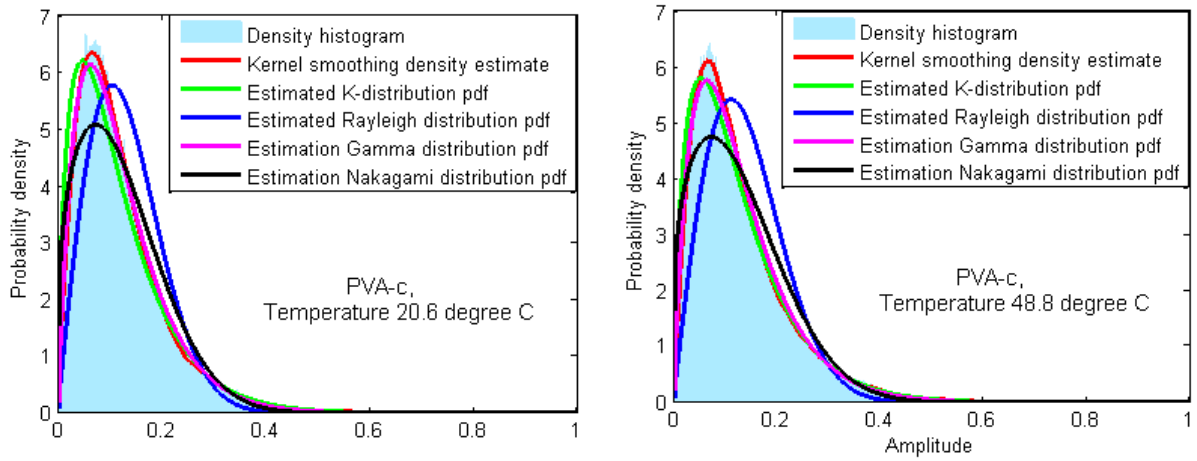

Figure 11. The Histogram designated for empirical data, registered with the PVA-c phantom for initial and maximum temperature. and fitting probability density functions designated (K- distribution, Rayleigh, Gamma and Nakagami distribution).

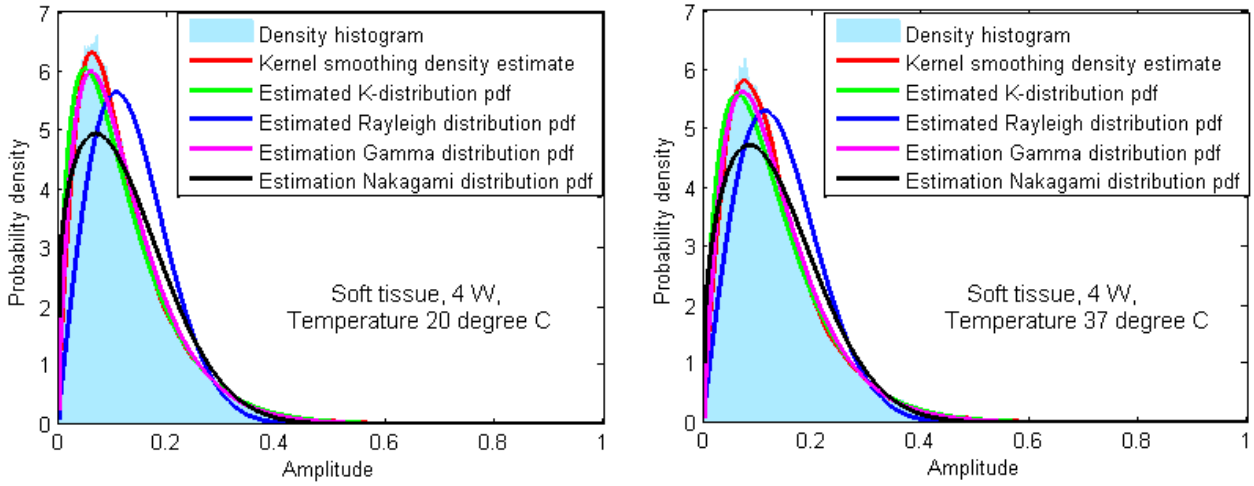

Figure 12. The Histogram designated for empirical data, registered with the soft tissue sample for initial and maximum temperature (of heating with power 4W) and fitting probability density functions designated (K-distribution, Rayleigh, Gamma and Nakagami distribution).

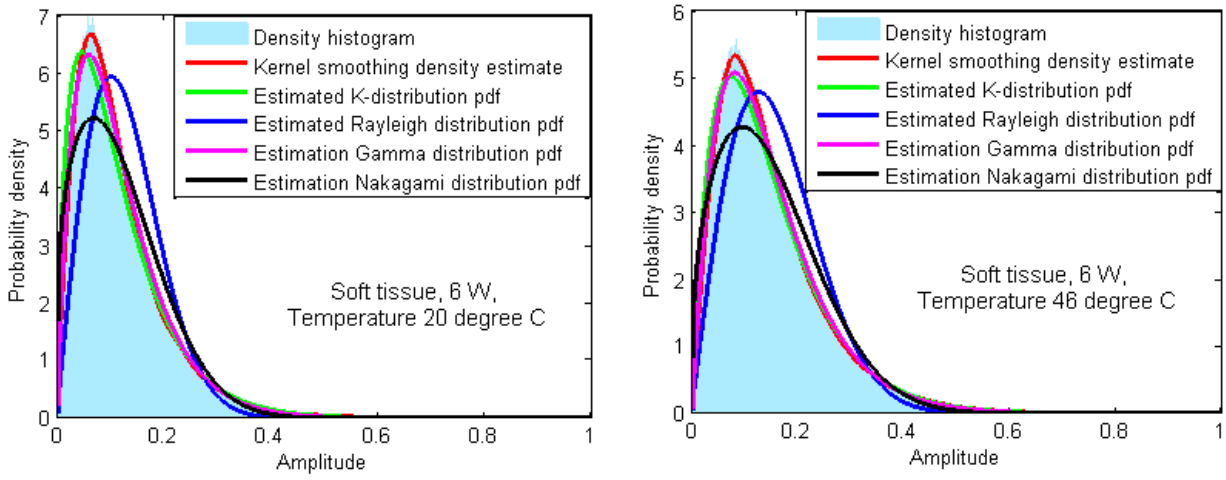

Figure 13. The Histogram designated for empirical data, registered with the soft tissue sample for initial and maximum temperature (of heating with power 6W) and fitting probability density functions designated (K- distribution, Rayleigh, Gamma and Nakagami distribution).

Table I. Mean square error (MSE), determined by comparing the different distributions of the empirical data at different times during the experiment with heating and cooling the PVA-C

Time, [x 0.5 min]	Rayleigh distribution	Gamma distribution	Nakagami distribution	K distribution
1	0.4027	0.0233	0.1714	0.1207
40	0.4887	0.0240	0.1791	0.1028
80	0.5188	0.0331	0.2165	0.0991
120	0.5150	0.0288	0.1914	0.0670
140	0.4622	0.0268	0.1785	0.0663
180	0.4223	0.0237	0.1625	0.0597
220	0.4366	0.0223	0.1657	0.0647
240	0.4483	0.0264	0.1668	0.0647
320	0.4438	0.0287	0.1899	0.1049
360	0.4433	0.0284	0.1859	0.0956

Table II. Mean square error (MSE), determined by comparing the different distributions of the empirical data at different times during the experiment with heating and cooling the soft tissue (4 W)

Time, [x 5 s]	Rayleigh distribution	Gamma distribution	Nakagami distribution	K distribution
1	0.4901	0.0133	0.1734	0.056
60	0.3526	0.0125	0.1462	0.0414
120	0.3030	0.0114	0.1338	0.0512
180	0.3890	0.0152	0.1631	0.0498
240	0.3929	0.0153	0.1631	0.0528

Table III. Mean square error (MSE), determined by comparing the different distributions of the empirical data at different times during the experiment with heating and cooling the soft tissue (6 W)

Time, [x 5 s]	Rayleigh distribution	Gamma distribution	Nakagami distribution	K distribution
1	0.4656	0.0148	0.1868	0.0893
60	0.2763	0.0093	0.1159	0.0399
120	0.2675	0.0086	0.1177	0.0279
180	0.2962	0.0881	0.1228	0.0324
240	0.3397	0.0116	0.1396	0.0346

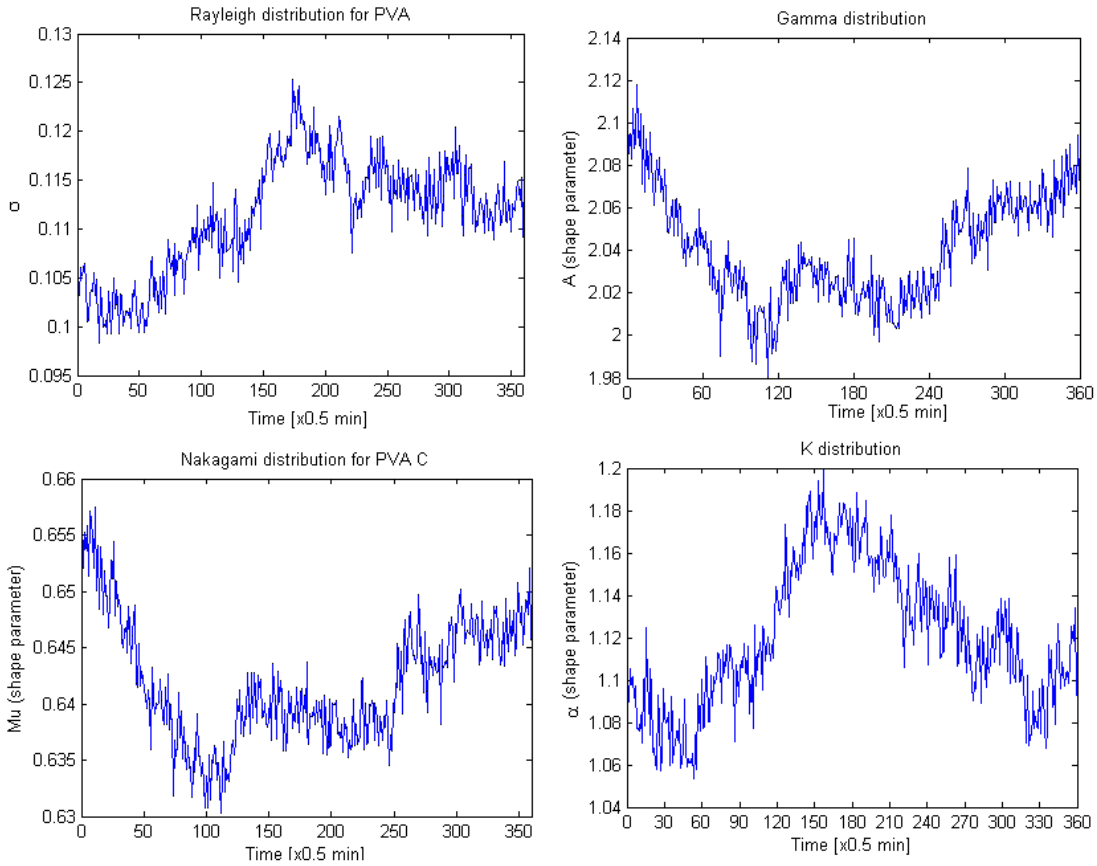

Figure 14. The parameter of distribution as a function of time from data for PVA-c sample (for Rayleigha, Gamma, Nakagami and K distribution)

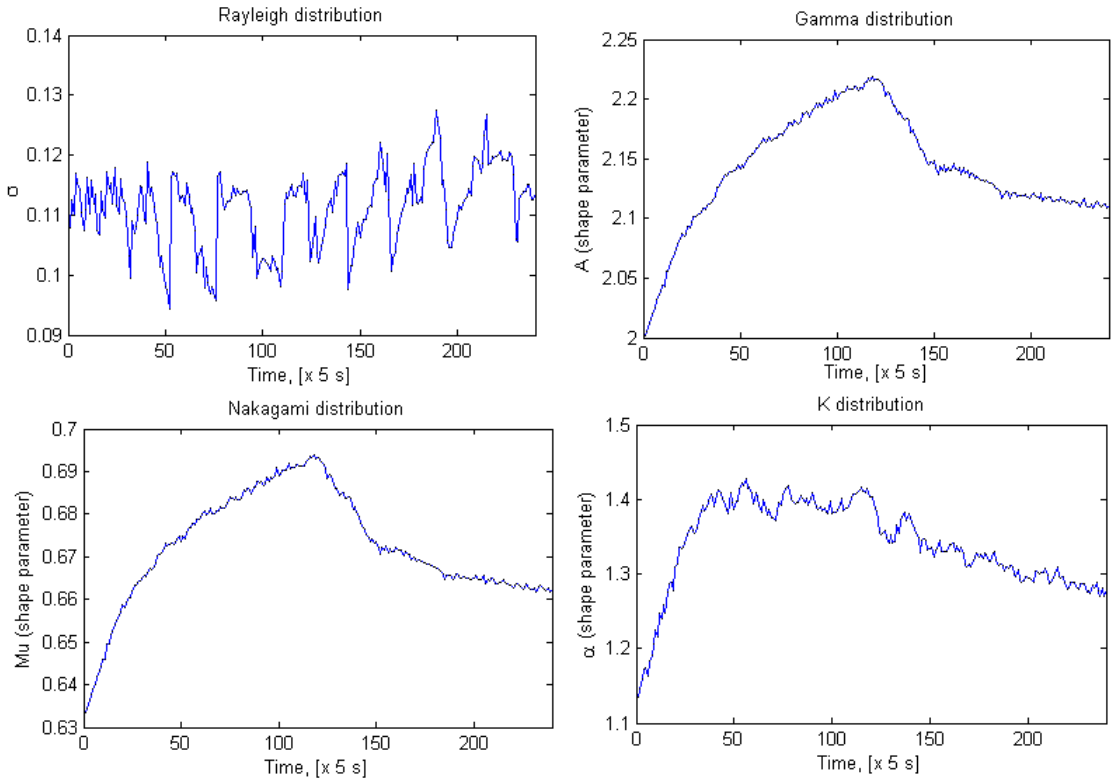

Figure 15. The parameter of distribution as a function of time from data for soft tissue sample (4W)

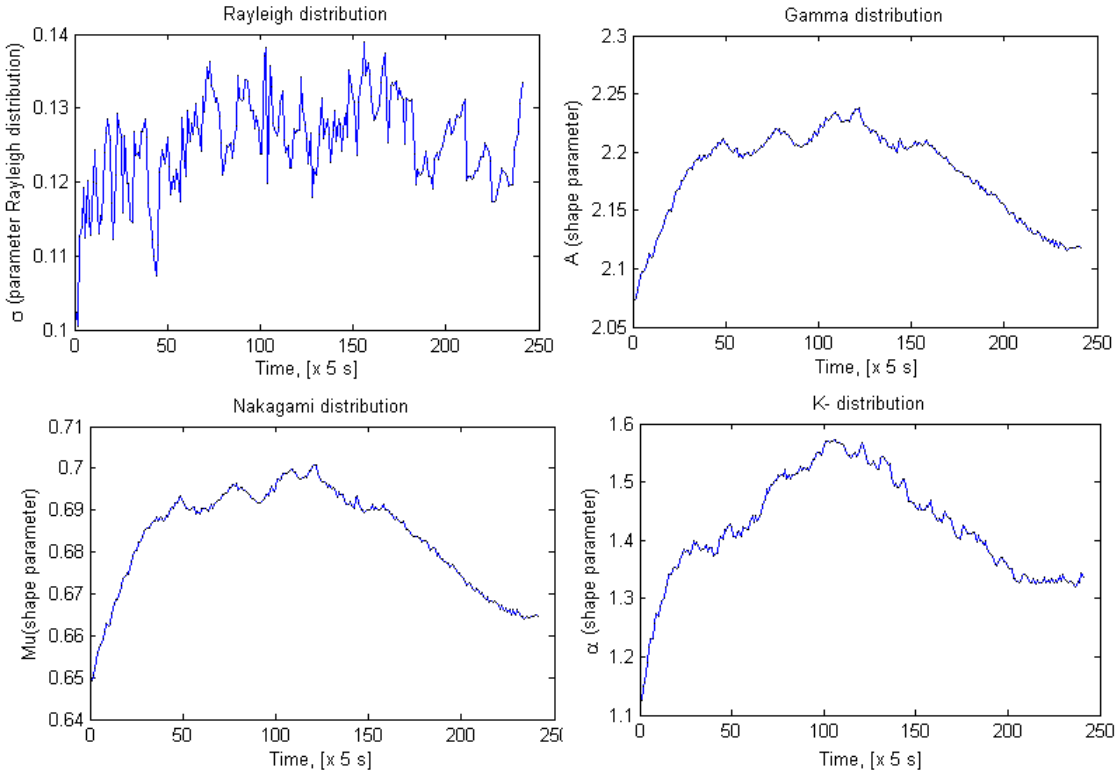

Figure 16. The parameter of distribution as a function of time from data for soft tissue sample (6W)

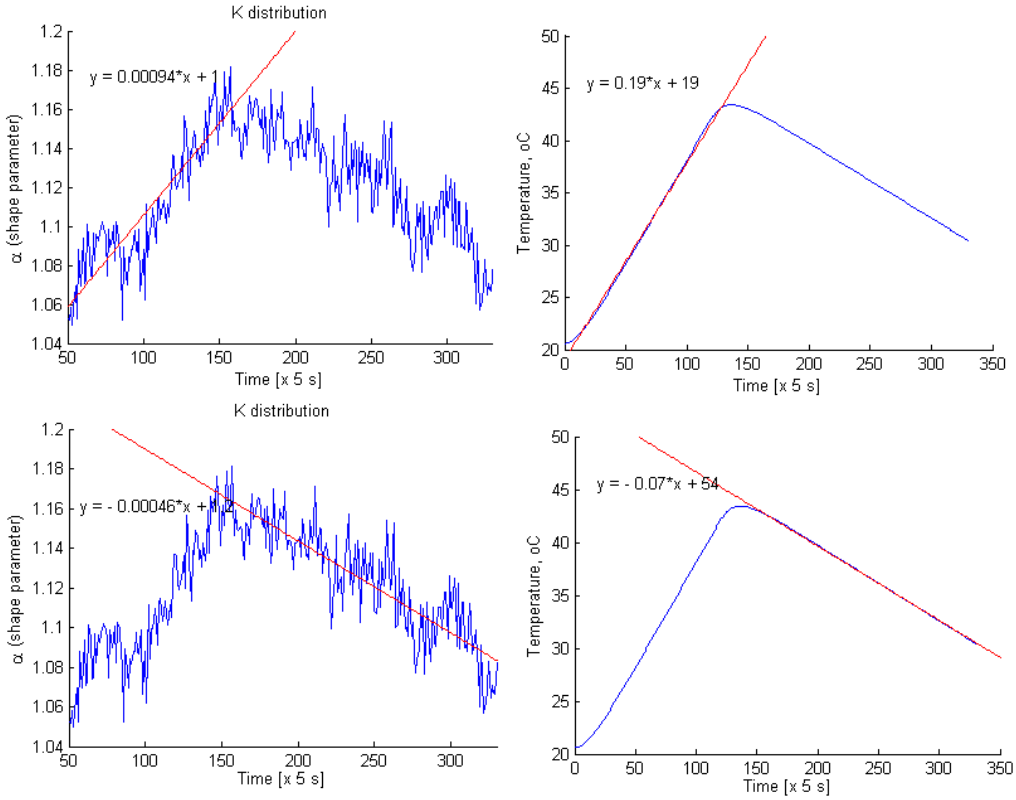

Figure 17. The parameter of distribution as a function of time from data for PVA-c phantom

Also the rate of changes of the shape parameter is nearly equal to the rate of measured temperature changes, cf. Fig. 17. Calculations are done for PVA-c phantom by linear regressions and calculations of ratio between measures of two different angles - for heating and for cooling processes:

$$\frac{tg\alpha}{tg\beta} = \frac{0.00094}{0.00046} \approx 2.04 \quad \text{and} \quad \frac{tg\alpha_1}{tg\beta_1} = \frac{0.19}{0.07} \approx 2.71 \qquad (5)$$

The links of the temperature changes during heating/cooling processes and the shape parameter changes are clearly visible in Fig. 18-19.

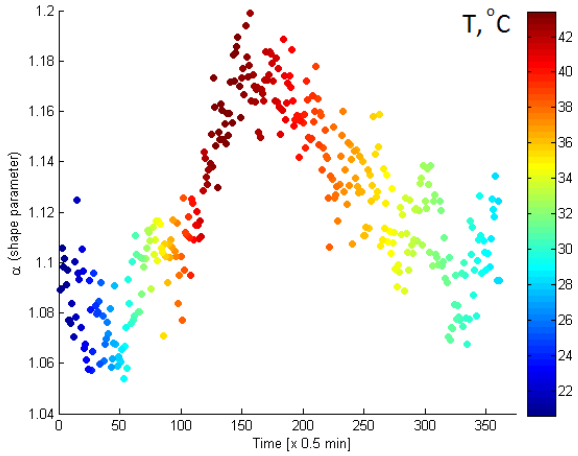

Figure 18. Time/temperature dependence shape parameter of K-distribution for PVA-c phantom.

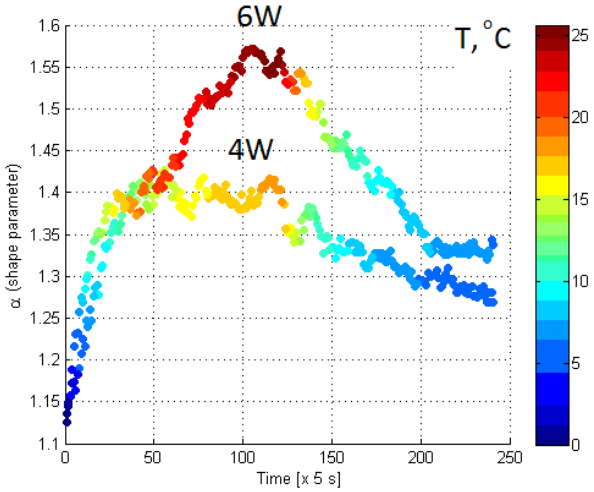

Figure 19. Time/temperature dependence shape parameter of K-distribution for soft tissue sample

Temperature changes in PVA-c sample the shape parameter of K-distribution is excellent temperature marker. The links of the rate of temperature increase/decrease and the rate of shape parameter changes are also in agreement with experimental measurement.

Thermal process for PVA-c sample proceeded slowly - one hour of heating, two hours of cooling than the process of heating the tissue sample *in vitro* - 10 minutes of heating and 10 minutes of cooling. The PVA was heated homogeneously by the immersing in the water bath whereas the soft tissue sample *in vitro* was heated locally inside its volume and the temperature distribution was strongly inhomogeneous. Nevertheless, the chosen by us shape parameter of K-distribution is a quite good temperature marker in the both cases. The differences in between the heating processes are responsible for the fact, that in the case of PVA-c sample we can measure by this parameter not only temperature level changes but also the rates of the heating/cooling process.

The results are very promising to elaborate in the near future new noninvasive method of temperature measurement inside soft tissues *in vivo*.

Acknowledgement

This work was partially supported by the National Science Centre (grant no. 2011/03/B/ST7/03347).

References

[1] F. Destrempes, G. Clouthier, A critical review and uniformized reprezentation of statistical distriction modeling the ultrasound echo envelope, Ultrasound in Med. & Biol., Vol. 36, No. 7 (2010) 1037–1051,.

[2] Quantitative Ultrasound in Soft Tissues. J. Mamou, M.L. Oelze (eds.), Springer 2013.

[3] B. Gambin, E. Kruglenko, T. Kujawska, M. Michaj³ow, Modeling of tissue in vivo heating induced by exposure to therapeutic ultrasound, Acta Physica Polonica A, 119 (2011) 950-956.

[4] B. Gambin, E. Kruglenko, Some aspects of numerical modeling of temperature increase due to ultrasound beam irrediation of rat liver, Hydroacoustics, 14 (2011) 99-110.

[5] B. Gambin, T. Kujawska, E. Kruglenko, A. Mizera, A. Nowicki, Temperature fields induced by low power focused ultrasound in soft tissue during gene therapy. Numerical Predictions and Experimental Results, Archives of Acoustics, 34, 4 (2009) 445-459.

[6] P. Karwat, J. Litniewski, W. Secomski, T. Kujawska, K. Krawczyk, E. Kruglenko, B. Gambin, A. Nowicki, Nieinwazyjne obrazowanie temperatury tkanki miêkkiej in vitro metod¹ analizy przemieszczenia ech ultradŸwiêkowych, 59th Open Seminar on Acoustics, Boszkowo 10-14.09.2012, 101-104.

[7] P. Karwat, J. Litniewski, W. Secomski, T. Kujawska, K. Krawczyk, E. Kruglenko, B. Gambin, Non-invasive imaging of thermal fields induced in soft tissues in vitro by focused ultrasound using analysis of ultrasonic echoes displacement, Proceeding of International Conference Biomedical Engineering- Kaunas University of Technology (2012) 66-72.

[8] E. Kruglenko, B. Gambin, RF signal amplitude statistics during temperature changes in tissue phantoms, Hydroacoustics, 17 (2014). (in print).

[9] O. Doubrovina, B. Gambin, E. Kruglenko, Temperature level and properties of wavelet approximations of backscattered ultrasound, Hydroacoustics, 17 (2014), (in print).